# Absence of a Holelike Fermi Surface for the Iron-Based $K_{0.8}Fe_{1.7}Se_2$ Superconductor Revealed by Angle-Resolved Photoemission Spectroscopy

T. Qian,[1] X.-P. Wang,[1] W.-C. Jin,[2] P. Zhang,[1] P. Richard,[1] G. Xu,[1] X. Dai,[1] Z. Fang,[1] J.-G. Guo,[1] X.-L. Chen,[1] and H. Ding[1]

[1]*Beijing National Laboratory for Condensed Matter Physics, and Institute of Physics, Chinese Academy of Sciences, Beijing 100190, China*

[2]*Department of Physics, Renmin University, Beijing 100872, China*

(Received 30 December 2010; published 3 May 2011)

We have performed an angle-resolved photoemission spectroscopy study of the new iron-based superconductor $K_{0.8}Fe_{1.7}Se_2$ ($T_c \sim 30$ K). Clear band dispersion is observed with the overall bandwidth renormalized by a factor of 2.5 compared to our local density approximation calculations, indicating relatively strong correlation effects. Only an electronlike band crosses the Fermi energy, forming a nearly circular Fermi surface (FS) at $M$ ($\pi$, 0). The holelike band at $\Gamma$ sinks ~90 meV below the Fermi energy, with an indirect band gap of 30 meV, to the bottom of the electronlike band. The observed FS topology in this superconductor favors ($\pi$, $\pi$) inter-FS scattering between the electronlike FSs at the $M$ points, in sharp contrast to other iron-based superconductors which favor ($\pi$, 0) inter-FS scattering between holelike and electronlike FSs.

DOI: 10.1103/PhysRevLett.106.187001 PACS numbers: 74.25.Jb, 71.18.+y, 74.70.Xa, 79.60.−i

The surprising discovery of superconductivity over 30 K in $K_xFe_{2-y}Se_2$, which does not contain a toxic arsenic element, has brought new excitement to the field of iron-based superconductivity [1]. The end member $KFe_2Se_2$ (0.5 doped electron per Fe) is the isostructural electron-doped counterpart of $KFe_2As_2$ (0.5 doped hole per Fe). Since $KFe_2As_2$ ($T_c \sim 3$ K) has only holelike Fermi surface (FS) sheets according to band calculations [2] and angle-resolved photoemission spectroscopy (ARPES) [3], it is possible for $KFe_2Se_2$ to have only electron FSs. This would be quite different from other iron-based superconductors with high $T_c$'s, which have both holelike and electronlike FSs quasinested via the ($\pi$, 0) wave vector [4–7]. Interband pair scattering between holelike and electronlike FSs is widely believed to be important to iron-based superconductivity [8–16]. Loss of one type of FS in general leads to a significant reduction of interband pair scattering, even in the case of nested FS sheets with the same carrier type. Accordingly, the disappearance of holelike FS pockets in $BaFe_{1.7}Co_{0.3}As_2$ [17] and of electronlike FS pockets in $KFe_2As_2$ [3] is accompanied by a strong suppression of $T_c$. The high $T_c$ of $K_xFe_{2-y}Se_2$ suggests that either there are hole pockets contrary to material expectations, or the most commonly proposed mechanism might be incomplete. Thus it is critical to clarify the FS topology of this new kind of iron-chalcogenide superconductor. Another significant aspect of this material is that it seems to emerge from an antiferromagnetic (AFM) insulating phase instead of a metallic spin-density-wave (SDW) parent state as in the cases of many other iron-based superconductors. A similar superconductor, (Tl, K) $Fe_{2-y}Se_2$, was recently reported to have a $T_c$ as high as 40 K [18] when $y \leq 0.12$, while becoming an AFM insulator when $y \geq 0.4$. The insulating phase for the possible parent compound (Tl, K) $Fe_{1.5}Se_2$, as in the high-$T_c$ cuprates, makes this material unique and important to study.

In this Letter, we present ARPES results on the band structure and the FS of superconducting $K_{0.8}Fe_{1.7}Se_2$ ($T_c \sim 30$ K) single crystals, and compare them to our local density approximation (LDA) band results. Our main finding is that there is only one type of FS sheet in this material. The hole bands at $\Gamma$ never cross the Fermi energy ($E_F$), while an electron band crosses $E_F$ and forms a nearly circular FS at $M$ ($\pi$, 0). In addition, an indirect band gap between the hole band and the electron band is observed. The observed bandwidth and Fermi velocity are renormalized by a factor of 2.5 compared to our LDA results, indicating a relatively strong correlation effect in this material. The implications of the distinct FS topology observed in this iron chalcogenide on its magnetic and superconducting properties will be discussed.

The single crystals of $K_{0.8}Fe_{1.7}Se_2$ (nominal concentration $K_{0.8}Fe_2Se_2$) used in this study were grown by the flux method, as described in Ref. [1]. Transport measurements indicate a superconducting onset temperature at 30 K and a transition width of 3 K. ARPES measurements were performed at the Institute of Physics, Chinese Academy of Sciences, using the He I$\alpha$ ($h\nu = 21.218$ eV) and He II$\alpha$ ($h\nu = 40.814$ eV) resonance lines. The angular resolution was set to 0.2°, while the energy resolution was set to 35 and 70 meV for the He I$\alpha$ and He II$\alpha$ measurements, respectively. Samples with a typical size of $\sim 1 \times 1$ mm$^2$ were cleaved *in situ* and measured at 40 K in a working vacuum better than $5 \times 10^{-11}$ Torr. The $E_F$ of the samples was referenced to that of a gold film evaporated onto the sample holder. Although ARPES is known to be surface sensitive, isostructural (Ba, K)$Fe_2As_2$ is found by LEED (low-energy electron diffraction) and STM (scanning

 

tunneling microscope) to have no surface reconstruction [19]. Moreover, the superconducting gap observed in (Ba, K)$Fe_2As_2$ by ARPES closes at the bulk $T_c$ and the FS volume obtained by ARPES satisfies Luttinger's theorem with the bulk carrier concentration. Thus it is likely that ARPES results on $K_{0.8}Fe_{1.7}Se_2$ will be also mostly representative of the bulk properties.

We start with a wide energy spectrum [Fig. 1(a)] that includes shallow core levels and the valence band using 40.814 eV photons. The strong peak at the binding energy of 17.55 eV coming from K 3$p$ is found at slightly smaller energy than the one observed in $Ba_{0.6}K_{0.4}Fe_2As_2$ [20]. In addition, there is a peak at 12 eV with an unknown origin. Figure 1(c) displays energy distribution curves (EDCs) along several high symmetry directions ($\Gamma$-$M$, $M$-$X$, $\Gamma$-$X$), as defined in Fig. 1(b). One distinct feature in this material is a large, broad and weakly dispersive peak located at 0.9 eV. While it could originate from the bottom of the Fe 3$d$ orbitals, the lack of dispersion rather suggests that it corresponds more likely to the large incoherent component of the Fe 3$d$ orbitals, as shown in Fig. 1(d). In fact, a LDA + DMFT (dynamical mean field theory) calculation on FeSe has found a lower Hubbard band around 1 eV due to strong correlation effects in iron selenide materials [21]. As with other iron-based superconductors, electronic correlations lead to a renormalization of the band structure. As shown in Fig. 1(d), our LDA band calculations capture several features emphasized by the intensity plot of the second derivative of EDCs along high symmetry directions. Our calculated bands have been shifted up by 170 meV to be consistent with the experimental electron doping, and then renormalized by a factor of 2.5. Both the calculations (at $k_z = 0$) and the experimental data suggest that an electronlike FS pocket emerges at the $M$ point, defined as $(\pi, 0)$ in the unfolded Brillouin zone (BZ). However, there exist obvious discrepancies between theory and experiment. The main one is the opposite energy shift between the hole and electron bands with respect to LDA results, namely, a downward shift for the hole band and an upward shift for the electron band. Such an electron-hole asymmetric shift could be caused by the correlation effect, which can renormalize the crystal field as well. We also note that it has been demonstrated to be evidence for a dominant interband coupling [22].

To investigate further the FS topology of this new superconductor, we next focus on the electronic band structure in the vicinity of the Fermi level. We display in Fig. 2(a) the ARPES intensity plot of a cut passing through the $M$ point. The intensity plot clearly shows that an electronlike band crosses the Fermi level. This is further supported by its second derivative along the energy direction, given in Fig. 2(b), as well as by the corresponding EDCs and momentum distribution curves (MDCs), which

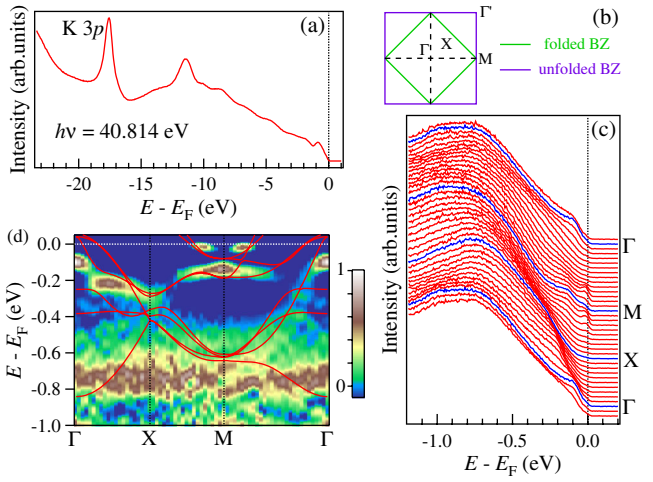


FIG. 1 (color online). (a) Photoemission spectra recorded with the He II$\alpha$ resonance line ($h\nu = 40.814$ eV) and integrated along $\Gamma$-$M$ within $\pm 15°$. (b) Schematic definition of the $\Gamma(0, 0)$, $M(\pi, 0)$ and $X(\pi/2, \pi/2)$ high symmetry points. Our notation refers to the unfolded Brillouin zone, which corresponds to the 1 Fe site/unit cell description. $\Gamma$-$M$ is along the Fe-Fe bond direction. (c) EDCs along several high symmetry directions recorded with the He I$\alpha$ resonance line ($h\nu = 21.218$ eV). Blue (dark gray) curves correspond to high symmetry points. (d) Second derivative intensity plot along high symmetry lines. The experimental data are compared to our LDA band structure calculations on $KFe_2Se_2$ ($k_z = 0$), which have been shifted up by 170 meV to account for the electron doping and then renormalized by a factor 2.5.

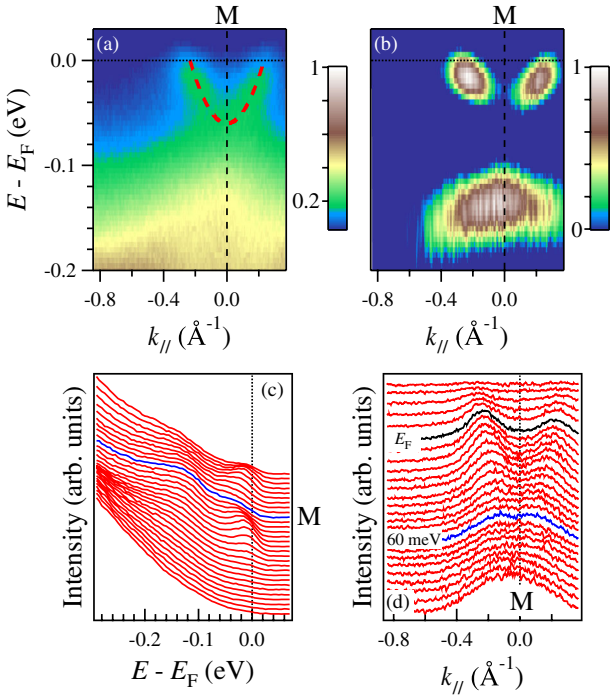


FIG. 2 (color online). (a) ARPES intensity plot along a cut passing through $M$ ($h\nu = 21.218$ eV). The red dashed curve is a parabola. The cut is indicated in Fig. 4(a) as a white line. (b)–(d) Corresponding second derivative intensity plot, EDCs, and MDCs, respectively.

are displayed in Figs. 2(c) and 2(d), respectively. From the EDCs and the MDCs, we estimate the bottom of the band at 60 meV. Taking into account this value, a simple parabolic fit allows us to estimate a Fermi velocity of 0.52 eV Å and an electron mass of $3.5m_0$. In addition to the electron band at the $M$ point, the data indicate the presence of a holelike band feature topping at $M$ around 130 meV below $E_F$.

In contrast to the $M$ point, we do not see any band crossing the Fermi level at the $\Gamma$ point. This is well illustrated by the ARPES intensity plot shown in Fig. 3(a). Instead, both the corresponding EDCs and second derivative intensity plot shown in Figs. 3(b) and 3(c), respectively, indicate a holelike band topping 90 meV below $E_F$. Interestingly, this value corresponds to a binding energy higher than the bottom of the electronlike band at the $M$ point, indicating an indirect band gap of 30 meV in the band structure. We speculate that this band gap might be related to the presence of an insulating phase at lower electron doping [18]. To check whether the top of the holelike band at the $\Gamma$ point can cross $E_F$ at a different $k_z$ value, we contrast the He I$\alpha$ (21.218 eV) data with data recorded with the He II$\alpha$ (40.814 eV) line [Fig. 3(d)], which are associated to a different $k_z$. The data are quite similar, except for a slight shift of the top of the band towards higher binding energies. We also plot in Fig. 3(e) the data obtained with the He II$\alpha$ line at the second folded BZ center $\Gamma'$ $(\pi, \pi)$, for which $k_z$ also varies. Once more, the holelike band does not cross the Fermi level. Using the conversion equation $k_z = \sqrt{2m[(h\nu - \phi - E_B)\cos^2\theta + V_0]}/\hbar$, where the effective work function $\phi$ is 4.4 eV and the inner potential $V_0$ is estimated to be about 15 eV in pnictides [23], we estimate the $k_z$ values to be about 3.2, 4.1, and 3.7 $(4\pi/c)$ for Figs. 3(c)–3(e), respectively [24].

The ARPES intensity map integrated in the $\pm 20$ meV energy range is given in Fig. 4(a). The high intensity regions define the Fermi surface. As explained above, while one electron FS pocket is detected at the $M$ point, there is no FS pocket observed at the BZ center. Although our experimental resolution does not allow us to resolve two electronlike FS pockets at the $M$ point, all band calculations [2,25–27] as well as previous ARPES measurements on similar iron-based superconductors [5,6] suggest that there should be two. As a first approximation, it is thus a reasonable assumption to consider that there are indeed two electronlike FS pockets at $M$ and that they are almost degenerate. The size of one electronlike FS pocket is estimated at 5.5% of the folded BZ. Assuming a double

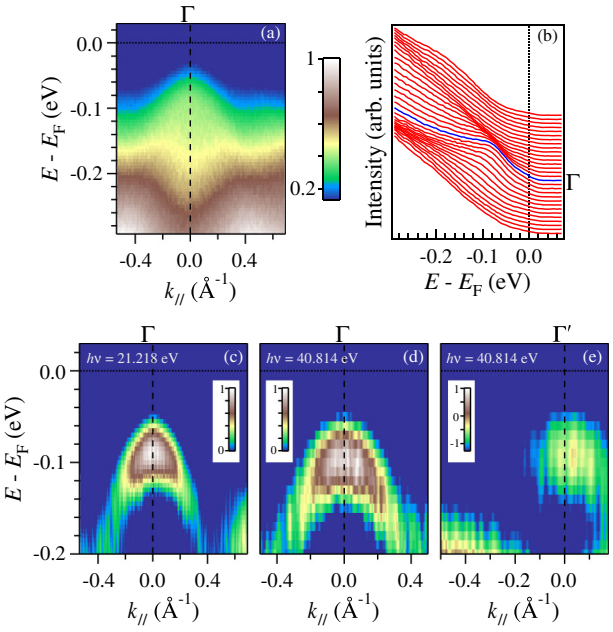


FIG. 3 (color online). (a) ARPES intensity plot recorded with the He I$\alpha$ resonance line ($h\nu = 21.218$ eV) along a cut passing through $\Gamma$ [$k_z = 3.2$ $(4\pi/c)$]. (b) EDCs along the cut shown in (a). (c) Second derivative intensity plot of the cut shown in (a). (d) and (e) correspond to second energy derivative intensity plot recorded with the He II$\alpha$ resonance line ($h\nu = 40.814$ eV) along a cut passing through $\Gamma$ [$k_z = 4.1$ $(4\pi/c)$] and $\Gamma'$ $(\pi, \pi)$ [$k_z = 3.7$ $(4\pi/c)$], respectively.

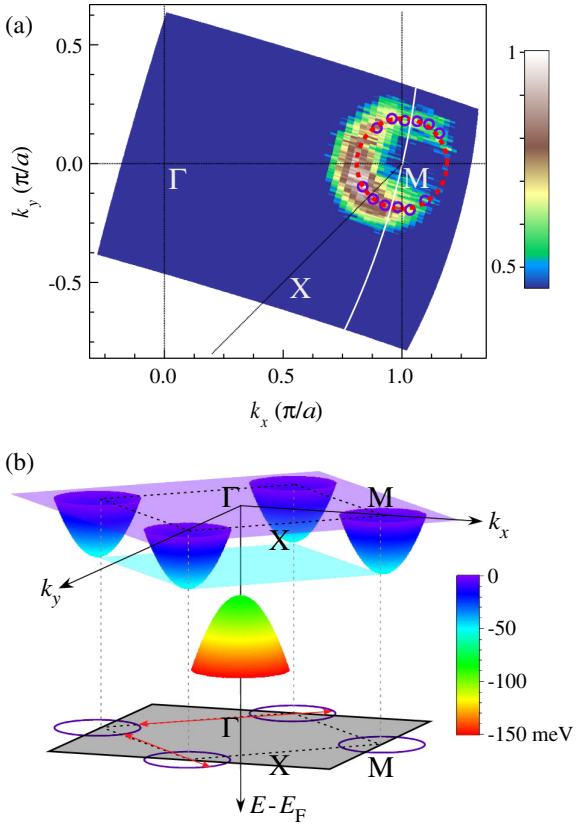


FIG. 4 (color online). (a) ARPES intensity mapping recorded with $h\nu = 21.218$ eV photons and integrated within $\pm 20$ meV with respect to $E_F$. (b) Schematic diagram summarizing the electronic band structure of $K_{0.8}Fe_{1.7}Se_2$ and illustrating the $(\pi, \pi)$ scattering processes.

degeneracy, this leads to an electron concentration of 11% per Fe, in good agreement with the chemical formula of the bulk material.

The observed FS topology in $K_{0.8}Fe_{1.7}Se_2$ is apparently in direct contradiction with the scenario promoting $(\pi, 0)$ AFM scattering between $\Gamma$-centered holelike and $M$-centered electronlike FS pockets as the key ingredient for Cooper pairing in iron-based superconductors [4–17,20]. However, we point out that even though $(\pi, 0)$ interpocket scattering fails to explain superconductivity as high as 30 K in the absence of holelike FS pocket at the zone center, interband scattering remains possible, albeit with a different wave vector. In fact, this can be viewed from Fig. 4(b) where the circular electronlike FSs at $M$ are connected by the $(\pi, \pi)$ wave vector in the unfolded BZ. Such inter-FS scattering is believed to favor opposite signs of the pairing order parameter on the two connected FSs [10–16]. The inequivalent Se sites fold the BZ with respect to the same $(\pi, \pi)$ wave vector. As a consequence of folding, there are two bands almost degenerated at the $M$ point, which should have different orbital characters. While a strong spin coupling constant between second iron neighbors ($J_2$) favors $(\pi, 0)$ AFM scattering, checkerboard AFM ordering and $(\pi, \pi)$ AFM scattering are favored by a strong coupling between nearest iron neighbors ($J_1$). Assuming that itinerant carriers are responsible for the pairing, the latter scenario is compatible with the observed FS topology. We caution that in such a case the current ARPES results do not allow us to distinguish between phonon-driven intraband scattering and AFM interband scattering. However, different superconducting pairing symmetries are expected for these two scenarios. Interestingly, Kuroki *et al.* predicted that although a $s_{\pm}$ paring symmetry is expected when both $\Gamma$-centered holelike and $M$-centered electronlike FS pockets are present, the absence of a holelike FS pocket at $\Gamma$ would favor a $d_{x^2-y^2}$ pairing symmetry in the unfolded BZ [11].

In conclusion, our ARPES results show that while an electron band crosses $E_F$ and forms a nearly circular FS at the $M$ $(\pi, 0)$ point, a hole band at the $\Gamma$ point never crosses $E_F$. The Luttinger volume of the electron FSs is ~11% of the BZ area assuming a double degeneracy, in agreement with the valence counting. An indirect band gap of ~30 meV between the top of the hole band and the bottom of the electron band is also observed, suggesting a band-insulating state at lower electron doping levels. Our LDA results on $KFe_2Se_2$ capture many dispersive features observed by ARPES when normalized by a factor of 2.5, indicating a relatively strong correlation effect in this material. Unlike many other iron-based superconductors where $(\pi, 0)$ scattering between holelike FSs at $\Gamma$ and electronlike FSs at $M$ is believed to dominate, this iron-based superconductor would likely favor $(\pi, \pi)$ inter-FS scattering between the electronlike FSs at $M$ if we assume an itinerant electron picture.

This work was supported by grants from Chinese Academy of Sciences (2010Y1JB6), Ministry of Science and Technology of China (2010CB923000) and Chinese National Science Foundation (11004232 and 11050110422).

[1] J.-G. Guo *et al.*, Phys. Rev. B **82**, 180520(R) (2010).
[2] G. Xu *et al.*, Europhys. Lett. **84**, 67015 (2008).
[3] T. Sato *et al.*, Phys. Rev. Lett. **103**, 047002 (2009).
[4] H. Ding *et al.*, Europhys. Lett. **83**, 47 001 (2008).
[5] K. Nakayama *et al.*, Europhys. Lett. **85**, 67 002 (2009).
[6] K. Terashima *et al.*, Proc. Natl. Acad. Sci. U.S.A. **106**, 7330 (2009).
[7] K. Nakayama *et al.*, Phys. Rev. Lett. **105**, 197001 (2010).
[8] P. Richard *et al.*, Phys. Rev. Lett. **102**, 047003 (2009).
[9] A. D. Christianson *et al.*, Phys. Rev. Lett. **101**, 157004 (2008).
[10] I. I. Mazin *et al.*, Phys. Rev. Lett. **101**, 057003 (2008).
[11] K. Kuroki *et al.*, Phys. Rev. Lett. **101**, 087004 (2008).
[12] F. Wang *et al.*, Phys. Rev. Lett. **102**, 047005 (2009).
[13] M. M. Korshunov and I. Eremin, Phys. Rev. B **78**, 140509 (R) (2008).
[14] K. Seo, B. A. Bernevig, and J. Hu, Phys. Rev. Lett. **101**, 206404 (2008).
[15] Z. J. Yao *et al.*, New J. Phys. **11**, 025009 (2009).
[16] V. Cvetkovic and Z. Tesanovic, Europhys. Lett. **85**, 37 002 (2009).
[17] Y. Sekiba *et al.*, New J. Phys. **11**, 025020 (2009).
[18] M.-H. Fang *et al.*, Europhys. Lett. **94**, 27 009 (2011).
[19] V. B. Nascimento *et al.*, Phys. Rev. Lett. **103**, 076104 (2009).
[20] H. Ding *et al.*, J. Phys. Condens. Matter **23**, 135701 (2011).
[21] M. Aichhorn *et al.*, Phys. Rev. B **82**, 064504 (2010).
[22] L. Ortenzi *et al.*, Phys. Rev. Lett. **103**, 046404 (2009).
[23] Y.-M. Xu *et al.*, Nature Phys. **7**, 198 (2011).
[24] The $k_z$ value varies with $V_0$ at a rate of ~0.05 $(4\pi/c)$ per eV.
[25] D. J. Singh and M.-H. Du, Phys. Rev. Lett. **100**, 237003 (2008).
[26] H.-J. Zhang *et al.*, Chin. Phys. Lett. **26**, 017401 (2009).
[27] F. Ma and Z.-Y. Lu, Phys. Rev. B **78**, 033111 (2008).